

NASA Technical Memorandum 100127

High Power Ion Thruster Performance

(NASA-TM-100127) HIGH POWER ION THRUSTER
PERFORMANCE (NASA) 14 p CSCL 21C

N88-12542

G3/20 UNCLAS
0111319

Vincent K. Rawlin and Michael J. Patterson
Lewis Research Center
Cleveland, Ohio

Presented at the
Fourth Symposium on Space Nuclear Power Systems
cosponsored by the Institute for Space Nuclear Power Studies
and the American Nuclear Society
Albuquerque, New Mexico, January 12-16, 1987

NASA

HIGH POWER ION THRUSTER PERFORMANCE

Vincent K. Rawlin and Michael J. Patterson
National Aeronautics and Space Administration
Lewis Research Center
Cleveland, Ohio 44135

SUMMARY

The ion thruster is one of several forms of space electric propulsion being considered for use on future SP-100-based missions. One possible major mission ground rule is the use of a single Space Shuttle launch. Thus, the mass in orbit at the reactor activation altitude would be limited by the Shuttle mass constraints. When the spacecraft subsystem masses are subtracted from this "available mass" limit, a maximum propellant mass may be calculated. Knowing the characteristics of each type of electric thruster allows maximum values of total impulse, mission velocity increment, and thrusting time to be calculated. Because ion thrusters easily operate at high values of efficiency (60 to 70 percent) and specific impulse (3000 to 5000 sec), they can impart large values of total impulse to a spacecraft. They also can be operated with separate control of the propellant flow rate and exhaust velocity. This paper presents values of demonstrated and projected performance of high power ion thrusters used in an analysis of electric propulsion for an SP-100 based mission.

INTRODUCTION

High specific impulse electric propulsion is a fuel efficient alternative to chemical propulsion for many missions and has been recommended by the National Commission on Space (NCOS) to build the 21st Century Bridge Between Worlds that will open the Solar System (NCOS 1986). However, high specific impulse electric propulsion requires large amounts of electric power to maintain reasonable thrusting times. The lack of large quantities of space electric power is one reason electric propulsion is not presently used for energetic missions. But the reality of the SP-100 space nuclear power system gives mission planners an opportunity to use advanced electric propulsion systems (Wiley et al. 1986). Specific applications of nuclear electric propulsion to near-earth (Buden and Garrison 1985 and Garrison 1982) missions appear in the literature. More recently, Hardy et al. (1987) have looked at SP-100-based mission capabilities provided by three types of electric propulsion. Those forms of electric propulsion included high power resistojets, arcjets, and ion thrusters. The current paper describes ion thruster operation and presents demonstrated and expected performance of high power ion thrusters used in that analysis for an SP-100-based mission.

APPARATUS

Figure 1 shows a mercury ion thruster, similar to that developed for NASA's Solar Electric Propulsion Stage (SEPS), and power processing used to operate the thruster (Lovell et al. 1979). As shown, the power processing has

been simplified from previous designs to operate with only five power supplies (Rawlin 1979). Here liquid mercury is vaporized, then ionized via bombardment by electrons which are emitted from the cathode and collected by the anode. The ions drift toward the screen grid of the ion accelerating system where they are electrostatically focused into beamlets and accelerated to a high exhaust velocity. Electrons from the neutralizer are then injected into the ion beam to prevent buildup of a positive space charge. When the propellant is initially a gas (as in the case of xenon or argon), the propellant vaporizers and power supplies are not needed. Two 30-cm diameter laboratory model ion thrusters, with different ionization chambers, have both been operated with mercury and inert gas propellants and input electric power levels to 22 kW using laboratory power supplies. The major differences between these ionization chambers are the strength and shape of the magnetic field used to increase the effective path length of the ionizing electrons. The SEPS thruster uses axial and radial (Alnico) magnets placed on the outer walls of the ionization chamber to provide a weak divergent magnetic field between the upstream cathode (located on axis) and the downstream end of the anode. The other ionization chamber utilizes very strong samarium cobalt magnets placed in rings on the upstream end and the cylindrical side wall such that the magnetic polarity of the rings alternate. With this geometry, the magnetic field is mostly at the ionization chamber boundaries. This ring-cusp configuration has been described in detail by Sovey (1982), Beattie and Kami (1982), and Patterson (1986).

The ion accelerating systems used for the tests herein were either SEPS hardware or similar laboratory equipment and consisted of two dished molybdenum electrodes separated by a spacing of about 0.6 mm. The diameters of the holes in the 0.38-mm thick screen and accelerator grids were 1.9 and 1.1 mm, respectively. The open area fractions of each grid were 0.67 and 0.24, respectively.

The ion thrusters were tested in a space simulation vacuum facility that was 4.6 m in diameter by 19.2 m long and had an operating pressure (ion thruster on) of about 3×10^{-3} Pa.

PROCEDURE

The 30-cm diameter ion thrusters were operated as described in Rawlin (1982) and the performance of the ionization chambers and ion accelerators were evaluated. Values of specific impulse, thrust, electric power, and thruster efficiency were calculated from steady-state electrical and propellant flow meters. The physical operating limits were identified and extended, where possible, to allow interpolation and extrapolation of thruster technology. Equations describing thruster performance were presented, simplified, and applied to 30-cm and larger 50-cm diameter ion thrusters.

ANALYSIS

Ion thruster performance is characterized by values of specific impulse (Isp), thrust (T), and input electric power (P) from which the efficiency of the thruster (EFFT) can be calculated as

$$EFFT = \frac{g I_{sp} T}{2P} \quad (1)$$

where g is the acceleration due to gravity (9.8 m/s^2), I_{sp} is in seconds, T is in newtons, and P is in watts.

The specific impulse of an ion thruster is defined here to be equal to the ratio of the thrust produced and the propellant weight flow rate and can be expressed as:

$$I_{sp} = \frac{K}{g} \sqrt{\frac{2e}{m}} (EFP) \sqrt{V_b} = 1.27 \times 10^3 \sqrt{\frac{V_b}{M}} \quad (2)$$

where K is a thrust loss factor accounting for beam ions which are multiply charged or have nonaxial trajectories. K typically has a value (assumed constant herein) of 0.95. The term e/m is the charge-to-mass ratio of singly charged ions and is related to M , the atomic mass of the propellant, which is expressed in a.m.u. EFP is the measured propellant efficiency, defined as the ratio of the ion beam current out of the thruster to the neutral propellant mass flow rate into the thruster expressed as a current of singly charged ions. For ion thrusters which have been optimized for a given propellant type and fixed operating point, EFP usually has a value between 0.9 and 1.0. A constant value of 0.94 was assumed for the SP-100 reference mission analyses. V_b is the beam voltage or net ion accelerating voltage, defined as the potential difference between the discharge chamber anode and the local ground, and determines the ion velocity. For the ion propulsion system analyses presented in Hardy (1987), the specific impulse was an input variable determined by an allowable range of V_b , which was 400 to 1800 V for the ion thruster baseline technology case discussed in detail later. Thrust is obtained from the ejection of ionized propellant (the thrust produced by lost neutral propellant is negligible) and may be expressed as:

$$T = K \sqrt{\frac{2m}{e}} J_b \sqrt{V_b} = 1.37 \times 10^{-4} J_b \sqrt{V_b M} \quad (3)$$

where J_b is the ion beam current in amperes. The maximum thrust from an electrostatic ion thruster is limited in three ways. One limit is the amount of ionized propellant that may be accelerated through the ion extraction grid holes. With a fixed total accelerating voltage (V_t , the potential difference between the discharge chamber plasma and the negative accelerator grid) the total ion current (J_b) may be increased, by increasing the discharge power, until the ionic space charge forces become appreciable compared to the grid electrostatic forces. When this occurs, an increasing fraction of the ions are unable to be focused through the negative accelerator grid holes and they impinge on that grid. Acceptable ion extraction system operation occurs at any value of beam current below this maximum. For normal operation, a 10 to 15 percent reduction below the space charge limit is typical. An empirical expression for the maximum beam current (J_{bmax}) from the SEPS thruster operated with a variety of propellants can be obtained from Rawlin (1982) and expressed as:

$$J_{bmax} = 4.73 \times 10^{-5} \frac{D^2}{\sqrt{M}} \left(\frac{V_b}{R} \right)^{2.2} \quad (4)$$

where D is the thruster beam diameter in meters and R is the ratio of net ion accelerating voltage (V_b) to the total ion accelerating voltage (V_t) and can be varied from about 0.2 to 0.9. The upper limit for R of about 0.9 is determined by the minimum value of the magnitude of the negative voltage on the second or accelerator grid. This voltage is required to prevent electrons in the neutralized ion beam from being attracted to the positive potentials upstream of the accelerator grid. The value of R can be reduced, using two-grid accelerating systems, to about 0.55. For a fixed grid geometry, beam-let divergence losses gradually increase (but are assumed constant herein by assuming an optimized geometry) with decreasing values of R until ion impingement on the accelerator grid becomes significant (Danilowicz 1973). At low values of R , these losses can also be minimized by improving ion focusing through the use of a third or decelerator grid placed downstream of the accelerator grid. This third grid is held at ground or neutralizer common potential and its use extends the range of R to values as low as 0.2 (Rawlin and Hawkins 1979). As can be seen by equations (3) and (4), a low value of R allows a higher value of J_{bmax} and, hence, higher thrust for a given V_b . However, this also leads to a higher value of V_t which, if greater than the assumed baseline value, would be considered a higher risk.

For the analyses conducted here and in Hardy (1987) the operational beam current was conservatively assumed to be about three-fourths of J_{bmax} . Using this expression for J_b , the equation for thrust becomes:

$$T = 4.85 \times 10^{-9} \frac{D^2 V_b^{2.7}}{R^{2.2}} \quad (5)$$

As equation (5) shows, thrust capability is independent of propellant type because thrust is proportional to $M^{0.5}$ while J_{bmax} is inversely proportional to $M^{0.5}$. A second limit of the maximum permissible beam current or thrust results from the maximum electric field which can be supported by the grid-to-grid spacing of the ion extraction system. SEPS thrusters have been operated with an electric field of 5×10^6 V/m, and a conservative value of 3.3×10^6 V/m was used here as the baseline operating condition. The third limit arises from thermal considerations when producing ions in the discharge chamber. Byers and Rawlin (1976) discuss this limit in detail for argon ion thrusters where the beam current and discharge power values are at least 80 percent greater than those which would be achieved with xenon and mercury propellants. The baseline operating conditions here are conservative and result in temperatures which are well below any thermal concerns.

Thruster input electric power may be expressed as:

$$P = J_b (V_b + EV) + P_f \quad (6)$$

where EV is an ionization power cost in watts per ampere of ion beam current and P_f is a small amount of power consumed during normal thruster operation for heaters (when necessary), plasma discharges to sustain the neutralizer and cathode, neutralizer to ion beam coupling losses, and accelerator grid impingement losses. For 30-cm diameter ion thrusters, operated on mercury or xenon, the value of EV typically ranges between 100 and 200 W per beam ampere (Patterson 1986 and Rawlin 1982). Therefore, a value of 150 W/A for EV was used in subsequent calculations. P_f was assumed to have a constant value

of 50 W, based on experimental results with 30-cm ion thrusters. Including these assumptions the thruster input power equation used in the analyses was:

$$P = J_b (V_b + 150) + 50 \quad (7)$$

This set of equations and the assumed ion thruster baseline technology parameters that are summarized in table I were used to project the performance of 30-cm and 50-cm diameter ion thrusters using mercury and xenon propellant.

RESULTS AND DISCUSSION

The results of applying the ion thruster baseline technology assumptions of table I to the thruster performance equations of the ANALYSIS section are discussed and compared with demonstrated thruster performance. In addition, the impact of improving certain thruster technology parameters is assessed.

Thruster Performance

Figure 2 shows calculated and demonstrated thrust as a function of specific impulse for 30-cm diameter ion thrusters operated both on mercury and xenon propellant. Calculations were made by applying the baseline technology assumptions to the equations presented earlier. The three data points shown on each calculated curve represent beam voltages from 400 to 1800 V. Thus, the values of thrust are constant for a given beam voltage. As shown by equation (5), thrust would be expected to vary with the square of the thruster diameter. Values of specific impulse vary inversely with the square root of the propellant atomic mass, as expected from equation (4). The ion beam current for each curve is constant (because the total accelerating voltage is constant); therefore, the power per thruster increases with specific impulse or beam voltage. At each calculated point a value for thruster input electric power is shown. The fraction of this total input power that is in the beam varies between 0.72 and 0.92; therefore, the sensitivity of variations in the assumed values of the ionization power cost (EV), the fixed power losses (Pf), the thrust loss factor (K), and the propellant efficiency (EFFP) would be expected to be minimal. Thrust varies linearly with specific impulse because only the beam voltage is being changed, and the square root of V_b appears in both the specific impulse and thrust expressions.

Figure 2 also compares the calculated thrust with demonstrated data obtained with 30-cm diameter thrusters. Only those data obtained with beam currents near the space charge flow limit and a baseline total accelerating voltage of 2000 V (± 500 V) are shown. Data above the calculated thrust line were obtained with total accelerating voltages between 2000 and 2500 V while those below the line had total voltages between 1500 and 2000 V. Previously presented data sources are identified by references. Some missions, such as those that are power limited, may not be able to utilize the full thrust capability. These thrusters can be operated to produce less thrust. At any value of specific impulse, the ion production may be decreased by reducing the ion production power and/or propellant flow rate, thereby reducing the ion beam current and thrust. Thus, values of thrust below those shown are assumed to be easily achievable. For mercury, the data at lower values of specific

impulse, were obtained with three grid optics while all of the data shown for xenon were taken with conventional two grid accelerating systems.

Projected and demonstrated values of thrust, specific impulse, and power are combined to give values of thruster efficiency (EFFT), which are shown in figure 3 as functions of specific impulse. The curves of calculated performance are independent of thruster size if the fixed power losses are neglected as can be seen by combining equations (1), (2), (3), and (7). Values of demonstrated thruster efficiency are for 30-cm diameter thrusters (except where noted) with divergent and ring cusp magnetic field discharge chambers. All of the data, except for those from Rawlin (1979), were obtained with two grid optics. The main reasons the mercury data fall below the calculated curve is that the propellant efficiency (EFFP) was, in actuality, a few percent less than that assumed and the ion production costs were about 30 percent greater than assumed. At low values of specific impulse (less than 3000 sec) the efficiency values of Rawlin (1982) drop off rapidly because the thruster was operated in a "deep throttle mode" where the propellant and power efficiencies are both below design values. With xenon, the ion production costs are lower; therefore, the major reason that most of the data fall below the calculated curve is that the actual propellant efficiency values were lower than that assumed. It should be noted that the single datum point for Beattie et al. (1985), which lies just above the calculated curve, was obtained with a thruster that was optimized for xenon propellant and employs the highest level of technology (hollow cathodes, ring cusp magnetic field, and three grid optics).

The location of each datum point is independent of input electric power level, which varies between 0.7 and 21.7 kW for the data shown.

Risk Versus Technology Level

The majority of ion thruster research has been with mercury propellant in ion thrusters using two grid optics and ranging in size from 5 to 150 cm in diameter. A 15-cm diameter thruster was tested in space for more than 10 years before the propellant supply was exhausted (Kerslake 1981). More recently, 8- and 30-cm diameter thrusters have been developed to states of flight (Power 1978) or technology (Lovell et al. 1979) readiness. These thrusters both use divergent magnetic field discharge chambers and closely spaced dished grids. Operation of thrusters at higher power levels and with inert gases has been demonstrated to be relatively straightforward (Rawlin 1982 and Patterson 1986) and, therefore, of relatively low risk when the total accelerating voltage is less than or equal to 2000 V. Industry has proposed to use a 25-cm diameter xenon ion thruster to provide the north-south station-keeping function of communication satellites at geosynchronous altitude (Beattie et al., 1985). That thruster, which operates with about 1.3 kW of input electric power, uses advanced thruster technology, such as a ring cusp magnetic field discharge chamber and three grid optics, and has demonstrated over 4300 hr of ground testing (Beattie et al. 1987).

For space missions that may have several hundred kilowatts of electrical power available for propulsion, it is desirable (from a system simplicity viewpoint) for each thruster to be able to process more power and to produce more thrust in the specific impulse range of interest (2000 to 5000 sec) than

can be achieved with the baseline technology assumptions. One way to accomplish this would be to increase the total accelerating voltage which would allow a greater beam current. Increasing the beam current leads to larger values of thrust and power per thruster as shown by equations (3) and (6) and fewer thrusters per system (Hardy et al. 1987). Figure 4 shows the projected thrust for a 30-cm diameter thruster as a function of the total accelerating voltage for a fixed value of beam voltage (1800 V). Operation at lower values of beam voltage concurrent with these higher values of total accelerating voltage would lead to lower values of R and necessitate the use of three grid optics which have demonstrated only limited operation at beam current levels over 2 A (Rawlin and Hawkins 1979) and would be considered higher risk. Values of input power and relative risk for each point are also shown. The authors realize that "risk" is subjective and use it here only to show how different technologies or operating conditions relate to the baseline assumptions. Potential development risk increases with total voltage because operation at higher beam current and thruster power levels has not been demonstrated for extended periods of time. Although operation at a total voltage of 3000 V has been, occasionally, demonstrated it is believed to be approaching the maximum electric field strength for closely spaced grids of the SEPS design.

Another way to increase the thrust and power per thruster is to increase the thruster diameter. Figure 5 shows how the thrust and power would be expected to increase with thruster size. Also shown is a datum point from Reader (1964) for a 50-cm diameter mercury ion thruster. There the total grid voltage was about 10 kV and the grid-to-grid spacing was about 15 times that presently used with dished grids. This resulted in a much lower beam current than could be obtained with closer spaced optics. Operation at high beam voltage (8800 V) or specific impulse (about 8500 sec) leads to reduced values of the thrust-to-power ratio as expected from the equations. Increasing the thruster diameter to 50 cm with state-of-the-art thruster technology (hollow cathodes, ring cusp magnetic field discharge chambers, and closely spaced dished optics) appear straightforward, and at this time it would probably be a moderate risk venture. The actual technology risks of combining the 50-cm thruster with high power density operation are unknown because no data are available. Thus, they are assumed, at this time, to be high.

Thruster Mass

The masses of advanced 30- and 50-cm diameter ion thrusters has been estimated to be 11.4 and 20.4 K, respectively, from Byers (1979). It was the opinion of those authors that advanced thrusters would operate at power densities similar to those proposed here, have a magnetic field configuration more complicated than the SEPS divergent field geometry, and have three grid optics. Because the ion thruster mass is small compared to other system components, highly accurate values are not required for the present analyses.

Thruster Lifetime

We believe that the present life-limiting mechanism for ion thrusters is sputtering damage or erosion of discharge chamber components, such as the

upstream side of the screen grid, by low energy ions. Sputtering is a mechanism whereby surface atoms are ejected after a momentum exchange with incident ions. Singly charged ions would be expected to have energies, in electron volts, approximately equal to the anode to screen grid potential difference (about 30 V). About 10 percent of the ions created in the discharge chamber are doubly charged and would be expected to have energies of about 60 eV. At these energies sputtering yields (in atoms sputtered per incident ion) are low (10^{-4} to 10^{-3}) and increase rapidly as the ion energies increase from about 30 to 100 eV. The screen grid erosion is a maximum at the center of the grid because the plasma density and the ratio of doubly to singly charged ions also exhibit maxima on the thruster axis. The erosion rate also varies with ion production rate (or beam current density) for a given ion energy (discharge voltage). Endurance tests of SEPS thrusters indicated screen grid lifetimes of nearly 30 000 hr may be achieved when the discharge voltage is 32 V and the beam current is 2 A (Bechtel et al. 1982). Screen grid lifetime was defined as the time to erode to half the original thickness. A 500 hr test of a SEPS thruster operated at an increased beam current of 3 A and a reduced discharge voltage of 28 V gave a screen grid erosion rate which was about half that of the SEPS baseline condition (Rawlin and Hawkins 1979). This occurred because of the strong dependence of sputter yield on ion energy, especially at the lower values of ion energy. An approximate calculation has indicated that a 30-cm diameter mercury ion thruster operating at beam current of 4.1 A (the value projected for the baseline technology assumptions of table I) and a discharge voltage of 28 V would have a screen grid lifetime nearly equal to that of the SEPS thruster. The beam current density projected by the analysis presented herein is constant for 30-cm and 50-cm diameter mercury ion thrusters and would be considered low risk (based on lifetime) for a six month (4300 hr) mission. The use of xenon propellant in ion thrusters designed for mercury leads to similar discharge operating conditions. In addition, the sputtering yields from surfaces bombarded with xenon ions are expected to be about double those for mercury ions suggesting that a xenon ion thruster operating at the conditions of table I would have a screen grid lifetime of about 15 000.

Measurement of the screen grid erosion rate in a 25-cm diameter xenon ion thruster, operated at a beam current of 1.45 A and a discharge voltage of 28 V, projects a lifetime (wear to half thickness) in excess of 25 000 hr (Beattie et al. 1985). The measurement technique used in those tests involved thin film erosion monitors which give results that are consistently conservative by about a factor of two (Beattie 1983). Using these facts a 3.5 times increase in xenon ion beam current, to the conditions of table I (5.1 A), would be expected to reduce the screen grid lifetime to about 14 000 hr. Therefore, even though high current xenon ion thrusters have not demonstrated long lifetimes, analyses indicate that the thruster lifetimes would greatly exceed the requirements of a six month mission.

CONCLUSIONS

Candidate ion thrusters have been described for propulsion of spacecraft with large amounts of available electrical power, such as those that might use an SP-100 nuclear reactor. A set of equations and technology level assumptions, which are based on experimental results, have been presented and used to predict the performance of ion thrusters as a function of specific impulse in the range of 2000 to 5000 sec. The projected results were compared

with demonstrated data and agreement was shown for a large range of operating conditions. Performance projections were made which show the impact of advanced technology assumptions on thrust and power capabilities of individual thrusters. Increased thrust and power per thruster allows fewer numbers of thrusters to be used which simplifies the propulsion system, especially when large power levels are available. The relative risk of advanced thruster technologies were compared to the low risk of the baseline technology assumptions and were discussed. Also briefly discussed was the expected lifetime of ion thrusters operating at thrust and power levels greater than those which have been demonstrated. The conclusions reached were that 30- or 50-cm diameter ion thrusters operated with mercury or xenon propellant should have lifetimes which are probably adequate for many near-Earth missions.

ACKNOWLEDGMENT

This work was performed at the National Aeronautics and Space Administration's (NASA) Lewis Research Center and supported by NASA's Office of Aeronautics and Space Technology under RTOP 506-42-31. Additional support and technical advice provided by the Nuclear and Thermal Systems Office at NASA's Lewis Research Center was greatly appreciated.

REFERENCES

1. J.R. Beattie and S. Kami, "Advanced Technology 30-cm Diameter Mercury Ion Thruster," AIAA Paper 82-1910, American Institute of Aeronautics and Astronautics (1982).
2. J.R. Beattie, "Endurance Test of a 30-cm-Diameter Engineering Model Ion Thruster," NASA CR-168132, Hughes Research Laboratories, CA (1983).
3. J.R. Beattie, J.N. Mattosian, R.L. Poeschel, W.P. Rogers, and R. Martinelli, "Xenon Ion Propulsion Subsystem," AIAA Paper 85-2012, American Institute of Aeronautics and Astronautics (1985).
4. J.R. Beattie, J.N. Mattosian, and R. R. ROBSON, "Status of Xenon Ion Propulsion Technology," AIAA Paper 87-1003, American Institute of Aeronautics and Astronautics (1987).
5. R.T. Bechtel, G.E. Trump, and E.L. James, "Results of the Mission Profile Life Test," AIAA Paper 82-1905, American Institute of Aeronautics and Astronautics (1982).
6. D. Buden and P.W. Garrison, J. Propulsion Power, 1, 70 (1985).
7. D.C. Byers, and V.K. Rawlin, "Electric Bombardment Propulsion System Characteristics for Large Space Systems," AIAA Paper 76-1039, American Institute of Aeronautics and Astronautics (1976). (NASA TM X-73554.)
8. D.C. Byers, F.F. Terdan, and I.T. Myers, "Primary Electric Propulsion for Future Space Missions," AIAA Paper 79-0881, American Institute of Aeronautics and Astronautics. (NASA TM-79141.)

9. R.L. Danilowicz, V.K. Rawlin, B.A. Banks, and E.G. Wintucky, "Measurement of Beam Divergence of 30-Centimeter Dished Grids," AIAA Paper 73-1051, American Institute of Aeronautics and Astronautics (1973). (NASA TM X-68286.)
10. P.W. Garrison, J. Spacecr. Rockets, 19, 534 (1982).
11. T. L. Hardy, V. K. Rawlin, and M.J. Patterson, "Electric Propulsion Options for SP-100 Reference Mission," NASA TM-88918, National Aeronautics and Space Administration (1987).
12. W.R. Kerslake, "SERT II Thrusters - Still Ticking After Eleven Years," AIAA Paper 81-1539, American Institute of Aeronautics and Astronautics (1981). (NASA TM-81774.)
13. R.R. Lovell, et al., "The 30-Centimeter Ion Thrust Subsystem Design Manual," NASA TM-79191, National Aeronautics and Space Administration (1979).
14. National Commission on Space, Pioneering The Space Frontier, Bantam Books, New York, p. 14 (1986).
15. M.J. Patterson, "Performance Characteristics of Ring Cusp Thrusters with Xenon Propellant," AIAA Paper 86-1392, American Institute of Aeronautics and Astronautics (1986). (NASA TM-87338.)
16. J.L. Power, "Planned Flight Test of a Mercury Ion Auxiliary Propulsion System. I - Objectives, Systems Descriptions, and Mission Operations," AIAA Paper 78-647-1, American Institute of Aeronautics and Astronautics (1978). (NASA TM-78859.)
17. V.K. Rawlin and C.E. Hawkins, "Increased Capabilities of the 30-Centimeter Diameter Hg Ion Thruster," AIAA Paper 79-0910, American Institute of Aeronautics and Astronautics (1979). (NASA TM-79142.)
18. V.K. Rawlin, "Reduced Power Processor Requirements for the 30-Centimeter Diameter Hg Ion Thruster," AIAA Paper 79-2081, American Institute of Aeronautics and Astronautics (1979). (NASA TM-79257.)
19. V.K. Rawlin, "Operation of the J-Series Thruster Using Inert Gas," AIAA Paper 82-1992, American Institute of Aeronautics and Astronautics (1982). (NASA TM-82977.)
20. P.D. Reader, "Experimental Performance of a 50-Centimeter Diameter Electron Bombardment Ion Rocket," AIAA Paper 64-689, American Institute of Aeronautics and Astronautics (1964).
21. C. Selph and D. Perkins, "An Analysis of Electromagnetic Thrusters for Orbit Raising," JSASS/AIAA/DGLR 17th International Electric Propulsion Conference, Tokyo, Japan, p. 580 (1984).
22. J.S. Sovey, J. Spacecr. Rockets, 21, 488 (1984).

23. R.J. Vondra, "A Review of Electric Propulsion Systems and Mission Applications," JSASS/AIAA/DGLR 17th International Electric Propulsion Conference, Tokyo, Japan, p. 600 (1984).
24. R.L. Wiley, A. D. Schmyer, J. A. Sholtis, Jr., R. L. Verga, and E.J. Wahlquist, "Space Reactor Power 1986: A Year of Choices and Transition," Advancing Toward Technology Breakout in Energy Conversion (21st IECEC), Vol. 3, p. 1411, American Chemical Society (1986).

Table I. - ION THRUSTER BASELINE TECHNOLOGY ASSUMPTIONS

Ion production:	
Thrust loss factor, K	0.95
Propellant efficiency, EFP	0.94
Ionization power cost, EV	150 W/A
Fixed power losses, Pf	50 W
Ion extraction:	
Total accelerating voltage, V	2000
Ratio of net-to-total accelerating voltage, R	
Three grid optics	0.2 to 0.55
Two grid optics	0.55 to 0.9

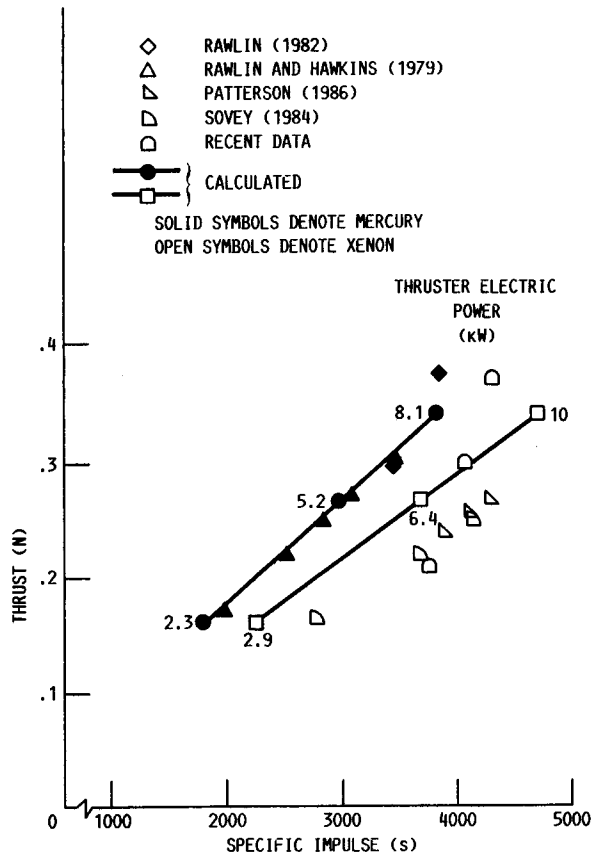


FIGURE 2. - THRUST FROM 30-CM DIAMETER THRUSTERS AS FUNCTIONS OF SPECIFIC IMPULSE AND PROPELLANT TYPE.

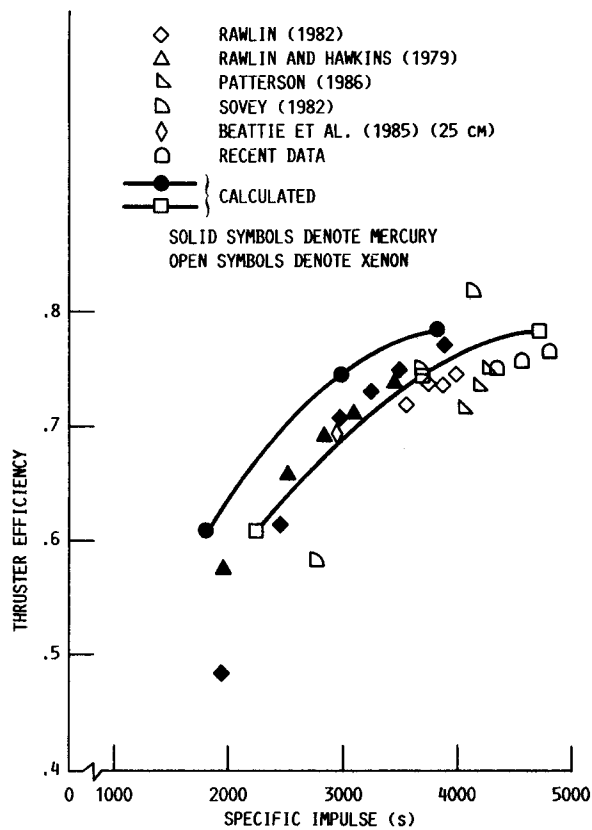


FIGURE 3. - THRUSTER EFFICIENCY AS FUNCTIONS OF SPECIFIC IMPULSE AND PROPELLANT TYPE.

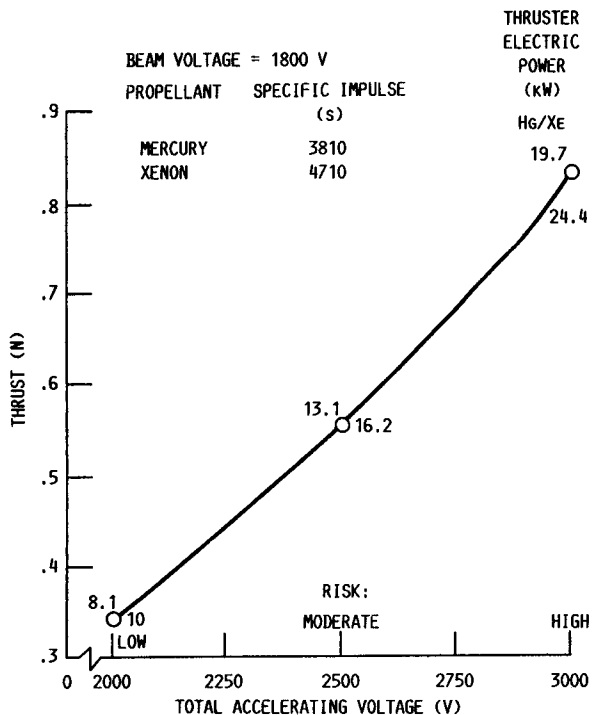


FIGURE 4. - THRUST FROM A 30-CM DIAMETER THRUSTER AS A FUNCTION OF TOTAL ACCELERATING VOLTAGE.

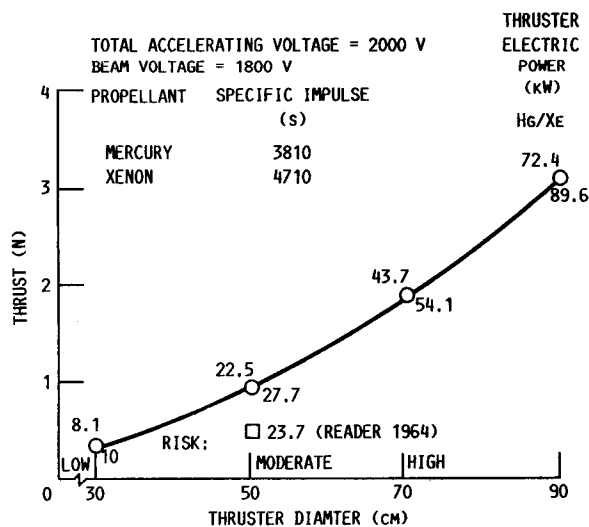


FIGURE 5. - THRUST AS A FUNCTION OF THRUSTER DIAMETER.



National Aeronautics and
Space Administration

Report Documentation Page

1. Report No. NASA TM-100127		2. Government Accession No.		3. Recipient's Catalog No.	
4. Title and Subtitle High Power Ion Thruster Performance				5. Report Date	
				6. Performing Organization Code	
7. Author(s) Vincent K. Rawlin and Michael J. Patterson				8. Performing Organization Report No. E-3676	
				10. Work Unit No. 506-42-31	
9. Performing Organization Name and Address National Aeronautics and Space Administration Lewis Research Center Cleveland, Ohio 44135-3191				11. Contract or Grant No.	
				13. Type of Report and Period Covered Technical Memorandum	
12. Sponsoring Agency Name and Address National Aeronautics and Space Administration Washington, D.C. 20546-0001				14. Sponsoring Agency Code	
15. Supplementary Notes Presented at the Fourth Symposium on Space Nuclear Power Systems, cosponsored by the Institute for Space Nuclear Power Studies and the American Nuclear Society, Albuquerque, New Mexico, January 12-16, 1987.					
16. Abstract The ion thruster is one of several forms of space electric propulsion being considered for use on future SP-100-based missions. One possible major mission ground rule is the use of a single Space Shuttle launch. Thus, the mass in orbit at the reactor activation altitude would be limited by the Shuttle mass constraints. When the spacecraft subsystem masses are subtracted from this "available mass" limit, a maximum propellant mass may be calculated. Knowing the characteristics of each type of electric thruster allows maximum values of total impulse, mission velocity increment, and thrusting time to be calculated. Because ion thrusters easily operate at high values of efficiency (60 to 70 percent) and specific impulse (3000 to 5000 sec), they can impart large values of total impulse to a spacecraft. They also can be operated with separate control of the propellant flow rate and exhaust velocity. This paper presents values of demonstrated and projected performance of high power ion thrusters used in an analysis of electric propulsion for an SP-100 based mission.					
17. Key Words (Suggested by Author(s)) Ion thruster Electric propulsion Nuclear electric propulsion			18. Distribution Statement Unclassified - Unlimited Subject Category 20		
19. Security Classif. (of this report) Unclassified		20. Security Classif. (of this page) Unclassified		21. No of pages 14	22. Price* A02